The zinc environment in Langmuir–Blodgett phospholipid multi-layers

Silvia Morante[a]*

[a]*Dipartimento di Fisica, Università di Roma* Tor Vergata *and Istituto Nazionale per la Fisica della Materia, Via della Ricerca Scientifica,1 00133 Roma Italy. E-mail: morante@roma2.infn.it*

The Zinc environment of a system formed by Langmuir-Blodgett phospholipid multi-layers is investigated by employing X-ray absorption spectroscopy. A comparative analysis of the Extended X-ray Absorption Fine Structure and Near Edge regions of the X-ray absorption spectra at the Zinc K-edge, in presence and in absence of the Myelin Basic Protein, clearly indicates that Zinc ions are bound to the heads of the phospholipidic molecules, while the presence of Myelin Basic Protein induces a visible distorsion of the geometry of the Zinc environment. These findings represent a first important step in understanding the interplay among the lipids of the myelin sheath, Myelin Basic Protein and Zinc, as Langmuir-Blodgett phospholipid multi-layers represent a valuable model for the multilamellar structure of the membrane surrounding the nerve axon.

1. Introduction

The myelin sheath is a rather unique multilamellar membrane formed by several lipid bilayers tightly wrapped around the nerve axon. Its integrity is crucial for the efficiency of the signal transduction along the axon. The Myelin Basic Protein (MBP) is known to play a crucial role in ensuring the stability of the myelin sheath (Boggs & Moscarello, 1982; Riccio *et al.*, 1986). There are also evidences (Cavatorta *et al.*, 1994) that Zn stabilizes the "in vitro" self-association of MBP dissolved in a phosphate buffer. To understand the role played by Zn in these aggregates one must, as a first step, get a precise information on the nature of the interaction of Zn ions with myelin sheath components.

X-ray Absorption Spectroscopy (XAS) is an ideal tool to obtain local information about the environment around specific atomic species in biological macromolecules. In this work I wish to report the first results of an investigation aimed at resolving the local geometry of Zn ions embedded in DLPA (Dilauroylphosphaditic acid) Langmuir-Blodgett multi-layers (LBML's) [1]. This system represents quite an accurate model of the multilamellar structure of the myelin sheath.

The analysis of the XAS spectra clearly shows that Zn ions are bound to the heads of the lipids, but the Zn environment is significantly different whether in presence or in absence of MBP, thus suggesting the existence of a yet to be understood interplay among Zn, MBP and LBML's.

2. Materials and Methods

Extensive X-ray absorption Spectroscopy (XAS) measurements have been performed at the General purpose Italian beam Line for Diffraction and Absorption (GILDA) of the European Synchrotron Radiation Facility (ESRF) in Grenoble (France) on a system formed by LBML's in presence or in absence of MBP [2] and in different pressure conditions, namely either in air or in a vacuum of about 10^{-5} bar. XAS spectra were recorded at room temperature, in fluorescence geometry. The X-ray absorption spectrum of Zn in a 10^{-3} M $ZnSO_4$ reference solution was also measured in fluorescence geometry.

3. Data analysis

To carry out an accurate phenomenological analysis of the data it is necessary to treat separately the XANES (X-ray Absorption Near Edge Structure) and the EXAFS (Extended X-ray Absorption Fine Structure) region of the XAS spectrum.

The analysis of EXAFS data was performed using the approach of (Benfatto *et al.*, 1986), implemented in the freely available GNXAS package (Filipponi *et al.*, 1995), which is based on a rigorous quantum-mechanical treatment of the signal, including single and multiple scattering effects. This approach has been successfully employed in study of the active site structure of various metallo-proteins (Zhang *et al.*, 1997; Meneghini & Morante, 1998).

4. Results

Not unexpectedly (Haas et al., 1994) the available space in between the heads of two adjacent layers depends on the hydration level of the sample. This in turn may affect the Zn binding geometry. This is the reason why we have performed XAS measurements in different pressure conditions (in air and in vacuum), as it is expected that changing the pressure indirectly modifies the level of LBML hydration. Hereafter for short we will denote the four samples on which we have performed our measurements using the following notation: $\mathbf{s}_a$, for LBML in absence of MBP, in air; $\mathbf{s}_b$, for LBML in absence of MBP, in vacuum; $\mathbf{s}_c$, for LBML in presence of MBP, in air and $\mathbf{s}_d$, for LBML in presence of MBP, in vacuum.

The XANES and the EXAFS regions of the four spectra are now discussed in turn.

4.1. XANES

In Fig. 1 the XANES region of the four spectra (left panel) together with their first derivative with respect to the photo-electron energy, $d\mu_{EXP}(E)/dE$ (right panel), are shown. A small, but significative shift in the edge energy is visible by comparing spectra in air and in vacuum ($\mathbf{s}_a$ *vs* $\mathbf{s}_b$ and $\mathbf{s}_c$ *vs* $\mathbf{s}_d$), as well as spectra at the same pressure ($\mathbf{s}_a$ *vs* $\mathbf{s}_c$ and $\mathbf{s}_b$ *vs* $\mathbf{s}_d$).

By looking at the first derivative of the spectra, it is clear that the edge energy shift is due to the systematic enhancement of a secondary shoulder in the pre-edge region that becomes more pronounced both by adding MBP and by lowering the pressure.

4.2. EXAFS

In Fig. 2 the experimental EXAFS structural signal, $\chi_{EXP}(k)$ (diamonds), superimposed to the total theoretical signal, $\chi_{TH}(k)$ (solid line), as it emerges from the GNXAS fitting procedure is shown separately for each one of the four measured samples. Experimental data as well as the function $\chi_{TH}(k)$ have been multiplied by k to compensate for their decrease with increasing k.

[1] A more detailed account of these and related experiments will be published elsewhere (Nuzzo *et al.*, 2000).

[2] LBML samples as well as MBP were prepared by H. Haas and P. Riccio.

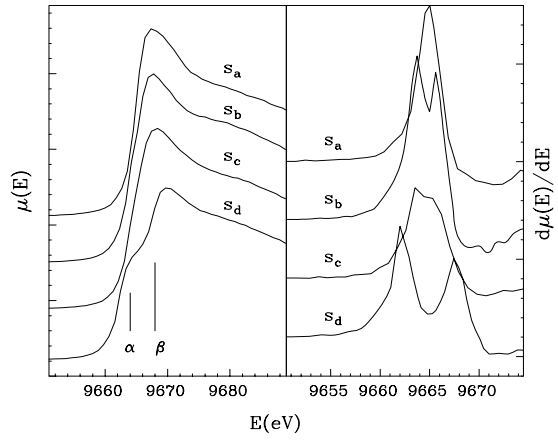

Figure 1
XANES region of the spectra (left panel) and their first derivative (right panel). The samples are labeled as explained in the text.

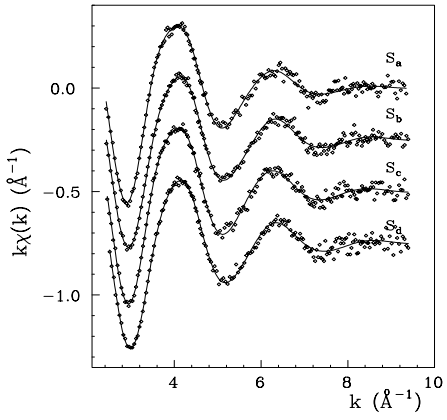

Figure 2
The experimental signal, $\chi_{EXP}(k)$ (diamonds) and the total theoretical signal, $\chi_{TH}(k)$, (solid line) for the four samples of Fig. 1.

Two irreducible 2-body contributions coming from two separate shells are necessary to adequately fit the data. The fitted parameters are shown in the Table. In the second, third and fourth column of the Table the values of the average distance, R_i, between the absorber (Zn) and the scatterers (oxygen), the corresponding Debye-Waller (DW) width, σ_i^2, and the multiplicity of the shell, N_i are reported for the two shells, $i = 1, 2$. Errors on all fitted parameters are on the last digit and are given in parenthesis. The two coordination shells are located at $R_1 \sim$1.95 Å and $R_2 \sim$3.4 Å from the Zn absorber, respectively. The fit also indicates that the first shell contains 4 oxygen atoms and the second only 1-2 oxygen atoms. In the last row of the Table for comparison we report the structural parameters obtained by fitting the data of the $ZnSO_4$ reference sample.

Table 1
Values of the parameters entering in the two-body signals, $\gamma^{(2)}$, from the fit to the four spectra and to the spectrum of the reference sample.

Sample	N_1	R_1 [Å]	$\sigma_1^2 x10^2$ [Å^2]	N_2	R_2 [Å]	$\sigma_2^2 x10^2$ [Å^2]
1	3.9 (3)	1.96 (2)	0.55(5)	1.3(2)	3.35(5)	1.1(2)
2	3.7 (3)	1.95 (2)	0.35(5)	1.4(3)	3.39(5)	1.0(2)
3	3.7 (3)	1.96 (2)	0.33(5)	1.5(3)	3.37(5)	1.3(2)
4	3.7 (3)	1.95 (2)	0.35(5)	1.3(2)	3.40(5)	1.1(2)
$ZnSO_4$	6.0 (4)	2.07 (2)	0.11(3)	2.9(2)	3.33(5)	1.5(2)

Comparing the values of the structural parameters of the four $\mathbf{s}_k$-samples with those of the hydrated Zn in the $ZnSO_4$ reference sample, we conclude that the atomic environment of Zn in LBML's is definitely different from that of Zn in water. The σ^2 values of the $\mathbf{s}_k$-samples are larger than those of the reference sample, indicating a stronger structural disorder of the Zn environment in the LBML medium.

5. Discussion

We have seen (see Sects. 4.1 and 4.2) that the XANES regions of the four $\mathbf{s}_k$-samples show significantly different structural features, while the EXAFS regions are quite similar, suggesting an almost identical short range atomic environment around the Zn. This fact excludes that the differences found in the XANES part of the spectra may come from differences in the coordination number or the chemical nature of the scatterers.

In LBML-MBP aggregates (Haas *et al.*, 1998) the protein is well packed in a sandwich-like structure of the type "headgroups-protein-headgroups", in which a small amount of water is also present. The head-head spacing in presence of the protein has been measured to be almost exactly the space occupied by the protein lying flat between the head-groups of the lipid matrix.

As in (Jacquament *et al.*, 1998), the behaviour of the shoulder visible in Fig. 1 is interpreted in term of a distorsion of the geometry of the Zn first coordination shell, or, more precisely, as a symptom of the progressive change from a tetrahedral to a planar geometry of the Zn bonds, which experimentally appears to be induced both by lowering the pressure and/or by adding MBP molecules to the LBML solution. The change in geometry can be explained as a consequence of steric hindrance experienced by the Zn ions due to the packing of phospholipid heads resulting both when the pressure is lowered and the MBP is added, because packing has the effect of reducing the physical space available to Zn ions.

The key question we have to address now is whether a direct Zn-MBP interaction, if present, could be detectable with the present technique. The interplay between Zn and MBP has been studied by fluorescence spectroscopy in (Cavatorta *et al.*, 1994), where the involvement of Histidine residues on Zn binding by MBP is conjectured. Notice that the MBP amino acidic sequence possesses the characteristic Zn-finger binding motif, His-X-X-His, thus, if Zn is bound to the protein, the by far most probable configuration should be the one in which Zn is bound to some of the available Histidines. The existence of this kind of binding should be easily detectable by XAS measurements. It is in fact well established experimentally (Strange *et al.*, 1987) that coordinated Histidines give rise to large multiple scattering contributions (from the nearby presence of Histidine imidazoles), producing a peak in the Fourier Transform (FT) at around 3.5 Å(Meneghini & Morante, 1998). As it is seen from the FT's of the four EXAFS spectra of Fig. 3, there is no evidence of any such enhancement in this region.

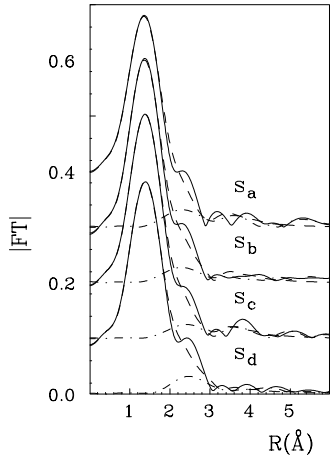

Figure 3
Modulus of the FT's of the four spectra: experimental (solid line), theoretical (dashed line) and differences between them (dot-dashed line).

However, the mere fact that this peak it is not visible does not exclude a direct binding of Zn to the MBP, because it may well be that the concentration of Zn atoms bound to MBP is too low in our experimental conditions to be detectable.

6. Conclusions

X-ray absorption spectroscopy studies of the Zn coordination mode in phospholipid LBML's in presence of MBP have been performed at the Zn K-edge. The combined detailed analysis of the XANES and EXAFS regions of the spectra has shown that coordination number, mean distance and DW factors do not show any visible change by adding the protein or lowering the pressure. Viceversa in both cases an increase in the height of a shoulder in the pre-edge region is clearly visible. This feature points to a change in the configuration of the scatterers around the Zn from a tetrahedral to a planar geometry. All our results consistently indicate that in all cases Zn ions are bound to the phosphatidic head groups of the lipids.

Although a modification of the geometrical environment of the Zn with the insertion of the protein is visible, new experiments are necessary in order to be able to detect a possible direct interaction between Zn and MBP.

Further studies in this direction are in progress (Nuzzo *et al.*, 2000). In particular the details of the interaction among Zn, MBP and LBML will be investigated through a new series of XAS experiments, which will exploit the potentialities of the REFLEXAFS set-up. REFLEXAFS is particularly useful in this case, as one can take advantage of the glancing incidence geometry, which effectively enhances concentration of the metallic ions in the sample, as they are seen to lie in an almost bidimensional medium. Measures will be carried out on two kinds of samples:

1) LBML's consisting of (negatively charged) DLPA molecules assembled in presence of both MBP and Zn, at a controlled pH around 8. In fact, it has been shown (Cavatorta *et al.*, 1994) that the influence of increasing the Zn concentration on the intensity of fluorescence spectrum of MBP in presence of phosphates shows a marked pH dependence. The observed behaviour suggests the involvement of the Histidine residues on the Zn binding process. It should be observed that, in order for the Histidines to be able to bind Zn, they should not be charged. This is the reason why the pH of the solution must be greater than 7.

2) LBML's made of neutral lipids. The aim of these meassurements is to check whether Zn can bind to neutral lipid heads.

Acknowledgements

I thank G.C. Rossi for reading the manuscript and V. Minicozzi for help in preparing the figures. I also wish to thank the scientific staff of the GILDA beamline. MURST and INFM are acknowledged for partial financial support.

References

Benfatto, M., Natoli, C.R., Bianconi, A., Garcia, J., Marcelli, A., Fanfoni, M.& Davoli, I.(1986). *Phys. Rev. B.* **34**, 5774–5781.
Boggs, J.M. & Moscarello, M.A. (1982). *In Lipid-Protein Interactions* **2**, 1–51. P.C. Jost and O.H. Griffith Editors. John Wiley and Sons, NY.
Cavatorta, P., Giovanelli, S., Bobba, A., Riccio, P., Szabo, A.G. & Quagliarello, E. (1994). *Biophys. J.* **66**, 1174–1179.
Filipponi, A., Di Cicco, A. & Natoli, C.R. (1995). *Phys. Rev. B* **52**, 15122–15134 and ibidem 15135–15149.
Haas, H., Torrielli, M., Steitz, R., Cavatorta, P., Sorbi, R., Fasano, A., Riccio, P. & Gliozzi, A. (1998). *Thin Solid Films.* **327-329**, 627–631.
Jacquament, L., Aberdam, D., Adrait, A., Hazemann, J.-L., Latour, J.-M. & Michaud-Soret, I. (1998). *Biochem.* **37**, 2654–2671.
Meneghini, C. & Morante, S. (1998). *Bioph. J.* **75**, 1953–1963.
Nuzzo, S., Cavatorta, P., Haas, H., Meneghini, C., Mobilio, S., Riccio, P. & Morante, S. (2000). In preparation.
Riccio, P.L., Masotti, L., Cavatorta, P., De Sanctis, A., Jetic, D., Bobba, A., Pasquali-Ronchetti, I. & Quagliarello, E. (1986). *Biochem. Biophys. Res. Commun.* **134**, 313–319.
Strange, R.W., Blackburn, P.F., Knowles, P.F. & Hasnain, S.S. (1987). *J. Am. Chem. Soc.* **109**, 7157–7162.
Zhang, H.H., Filipponi, A., Di Cicco, A., Scott, M.J., Holm, R.H., Hedman, B. & Hodgson, K.O. (1997). *J. Am. Chem. Soc.* **119**, 2470–2478.

 Received 31 July 2000 • Accepted 16 November 2000